Journal of Electroanalytical Chemistry 708 (2013) 13–19

Contents lists available at ScienceDirect

Journal of Electroanalytical Chemistry

journal homepage: www.elsevier.com/locate/jelechem

Simultaneous determination of methotrexate and calcium folinate with electrochemical method based on a poly-ABSA/functionalized MWNTs composite film modified electrode

Zuoyi Zhu [a], Fengli Wang [a], Fengmei Wang [b], Lingling Xi [a,*]

[a] Department of Chemistry, Xixi Campus, Zhejiang University, Hangzhou 310028, China
[b] Clinical Pharmacological Room of the Department of Pharmacy, Women's Hospital, School of Medicine, Zhejiang University, Hangzhou 310006, China

ARTICLE INFO

Article history:
Received 8 June 2013
Received in revised form 27 August 2013
Accepted 6 September 2013
Available online 19 September 2013

Keywords:
Electrochemical sensor
Functionalized multi-wall carbon nanotubes
Poly(*p*-aminobenzene sulfonic acid)
Methotrexate
Calcium folinate

ABSTRACT

A highly sensitive electrochemical sensor was fabricated by electropolymerizing *p*-aminobenzene sulfonic acid (ABSA) on quaternary amine functionalized multi-wall carbon nanotubes (Q-MWNTs) modified glassy carbon electrode (GCE). Q-MWNTs provide a conductive and stable network for the poly-ABSA (PABSA) immobilization. The voltammetric behaviors of methotrexate (MTX) and calcium folinate (CF) at the PABSA/Q-MWNTs/GCE were investigated by cyclic voltammetry (CV). Compared with bare GCE, Q-MWNTs/GCE and PABSA/GCE, the PABSA/Q-MWNTs/GCE exhibited excellent electrocatalytic oxidation toward MTX and CF. Separation of the oxidation peak potentials for MTX and CF was 0.26 V in phosphate buffer solution (pH 7.0), which made it suitable for simultaneous determination of these two compounds by differential pulse voltammetry (DPV). Under the optimized conditions, the anodic peak current of MTX was linear with the concentration from 0.1 to 8.0 μM in the presence of 8.0 μM CF, with a detection limit of 0.015 μM ($S/N = 3$). At the same time, the anodic current of CF was linear with the concentration from 0.1 to 6.5 μM with a detection limit of 0.020 μM in the presence of 8.0 μM MTX. The proposed sensor showed advantages of simple preparation, high sensitivity, good reproducibility and stability. It was successfully applied to simultaneous determination of MTX and CF in urine samples.

1. Introduction

Methotrexate (MTX), an antimetabolic agent, is an antifolate in a class of folic acid analogs that has demonstrated effective antineoplastic activity. It has been widely used in large doses for the treatment of acute lymphoblastic leukemia [1] and also as an effective antiinflammatory and immunosuppressive drug in low doses for the treatment of rheumatoid and other diseases [2–4]. Monitoring of the biological fluid MTX level is important for studies of efficacy, dosing schedules, different individual responses related to genetic polymorphism and adverse drug reactions.

Calcium folinate (CF), also known as leucovorin calcium, is a derivative of folic acid. This molecule is a natural compound occurring in living cells, where it plays a primary role in several metabolic pathways [5–7]. CF in the pharmaceutical industry is a drug used as vitamin against anemia and antidote to MTX. It has been in clinical use for many years as rescue agent following MTX therapy [8,9]. MTX induced toxicity can be prevented by using CF without diminishing its antitumor activity. Thus, fast and simple analytical methods are desirable for simultaneous determination of MTX and CF in biological samples.

A variety of methods exist that focus on the determination of MTX or CF. Fluorescence polarization immunoassay [10], radioimmunoassay [11], capillary electrophoresis (CE) [12] have been used to quantify MTX. There also have been high performance liquid chromatography (HPLC) methods with either UV or derivative fluorescence detection [13–15] for MTX determination. The reported analytical methods for CF were mainly based on HPLC in combination with gradient elution and UV or fluorescence detection [16,17]. CE with UV detection [18] and hyphenated techniques (LC–MS) [19] have been applied to simultaneous determination of MTX and CF.

Recently, interest has been increasing in the application of simple, sensitive, rapid and inexpensive electrochemical methods for the analysis of pharmaceutical drugs. These methods do not require tedious pretreatment and involve limited preseparation and consequently reduce the cost and time of analysis. In addition, electrochemical methods also help to identify the redox of drug compounds and provide important information about pharmacological actions. However, to the best of our knowledge, simultaneous determination of MTX and CF by the direct electrochemical methods has not been reported in any literature.

* Corresponding author. Tel./fax: +86 571 88273637.
E-mail address: xilingling@yahoo.com (L. Xi).

1572-6657/$ - see front matter © 2013 Elsevier B.V. All rights reserved.
http://dx.doi.org/10.1016/j.jelechem.2013.09.004

Therefore, the search of a reliable material for the electrode modification is of considerable interest for simultaneous determination.

Carbon nanotubes (CNTs) have been found to be an excellent modifier of chemically modified electrodes (CMEs) due to its unique properties [20]. Hence, CMEs based on CNTs have been widely used as they offer superior performance in terms of promoting electron-transfer, improving reversibility of electrochemical reaction and enhancing responses [21,22]. However, CNTs tend to aggregate in almost all kinds of aqueous and organic solutions. This property hampers the electrochemical studies and electroanalytical applications of CNTs. So far, most of the hitherto-developed strategies for preparing CNTs modified electrodes were based on the carboxyl group functionalization of CNTs or simply incorporating CNTs in Nafion [23–25], sodium dodecyl sulfate [26], hexadecyl trimethyl ammonium bromide [27], etc. From an electrochemical point of view, methods for the preparation of CNTs modified electrodes are still needed.

Conducting polymers also have been widely used as electrode modifiers for their good stability, ease of preparation, more active sites and homogeneity in the past two decades. Polymers based on aniline and aniline derivatives have been of particular interest due to their many desirable features such as facile preparation, environmental stability, and high conductivity. Recently, poly(*p*-aminobenzene sulfonic acid) (PABSA) modified electrodes have been reported for the electrochemical study of dopamine [28], uric acid [29], H_2O_2 [30], tyrosine [31], trifluoperazine [32], phenylephrine and chlorprothixene [33].

As far as we are aware no work on simultaneous determination of MTX and CF by electrochemical methods has been reported previously, this paper describes the construction, performance and application of a PABSA/MWNTs composite film modified electrode for simultaneous determination of MTX and CF. In this work, a kind of positively charged MWNTs with quaternary amine functionalization (Q-MWNTs), which had better hydrophilicity and dispersibility than MWNTs-COOH, was prepared to modify GCE. The cationic Q-MWNTs formed a rather uniform and stable film on the pre-anodized electrode surface via electrostatic interactions and could be a good matrix for hosting polymers. The electrochemical behavior of MTX and CF at the PABSA/Q-MWNTs/GCE exhibited much better electrochemical performance than that at bare GCE, Q-MWNTs/GCE and PABSA/GCE. By using differential pulse voltammetry (DPV), direct determination of MTX and CF in urine samples has been described. The sensor showed good reproducibility and stability for detection.

2. Experimental

2.1. Chemicals

MTX and CF were purchased from Aladdin Co. (Shanghai, China). 18-crown-6 ether and *p*-aminobenzene sulfonic acid were purchased from Aldrich (USA). MWNTs (⩾95%) with the average outer diameter about 20 nm were supplied by the Institute of Material Physics and Microstructure of Zhejiang University, China. All other chemicals used in this investigation were of analytical grade. The phosphate buffer solutions (PBS) at various pH values were prepared by mixing stock standard solutions of K_2HPO_4 and KH_2PO_4, and adjusted with 0.1 M HCl or NaOH. Deionized water employed in all experiments was obtained from a Millipore-Milli-Q system.

Stock solutions of MTX and CF were prepared at 1.0 mM with pH 7.0 PBS and stored at −20 °C. Exposure to direct sunlight was avoided. Urine samples were diluted 5-fold with deionized water.

2.2. Apparatus

The electrochemical measurements such as cyclic voltammetry (CV) and differential pulse voltammetry (DPV) were performed on the CHI 832 electrochemical work station (CH Instrument Co., Austin, TX, USA) with a conventional three electrodes system, which comprises a bare (3 mm i.d.) or modified GCE as working electrode, a Pt wire as counter electrode and a KCl saturated Ag/AgCl as reference electrode. Differential pulse voltammetry (DPV) was recorded from 0 to 1.0 V at a scan rate of 0.01 V s^{-1}, with pulse amplitude of 0.05 V, pulse period of 0.2 s and pulse width of 0.05 s. A Hitachi Scientific Instruments (London, UK) model S-3000H scanning electron microscope at an accelerating voltage of 15 kV was used for surface image measurements. Electrochemical impedance spectroscopy (EIS) was performed on the VMP2 potentiostat system (PARC Co., USA) in a frequency range of 100 kHz to 10 mHz with a peak to peak amplitude of 5 mV. All pH measurements were performed with a Suntex model SP-701 pH meter (Jiangsu, China).

2.3. Fabrication of the PABSA/Q-MWNTs/GCE

Q-MWNTs were prepared according to the method described in reference [34]. 5 mg of the obtained Q-MWNTs were dispersed in 10 mL deionized water and sonicated for 30 min, resulting in a rather homogeneous black suspension (0.5 mg mL^{-1}). Prior to surface modification, the GCE was polished with alumina slurry (0.05 μm) on a soft polishing cloth and cleaned by ultrasonication in ethanol and water successively. The GCE was anodized at +1.8 V for 240 s in 0.1 M $HClO_4$ and then successively scanned between +1.2 and +1.8 V until stable cyclic voltammograms (CVs) were obtained. The prepared anodized GCE was rinsed by water and dried in a nitrogen atmosphere. Then, 5 μL of the Q-MWNTs suspension was dropped directly onto the GCE (3 mm i.d.) surface. It was dried at ambient conditions to obtain the Q-MWNTs/GCE. PABSA was electrodeposited on the Q-MWNTs/GCE from a solution containing 0.01 M ABSA and 0.1 M H_2SO_4. Cyclic voltammetry was adapted for PABSA film growth between −1.5 and +2.0 V at a scan rate of 0.05 V s^{-1} for 5 cycles. After the polymerization, the electrode was treated in pH 7.0 PBS by repetitive scanning in the potential range of −1.0 and +1.0 V until a stable background was obtained. Thus, the PABSA/Q-MWNTs/GCE was obtained.

3. Results and discussion

3.1. Characteristics of Q-MWNTs

Fig. 1A shows the dispersed states of the Q-MWNTs and MWNTs−COOH in deionized water (1.0 mg mL^{-1}). Both were ultrasonicated in deionized water for 10 min. It was observed that Q-MWNTs dispersed much better compared with MWNTs−COOH, which completely settled down at the bottom of the vial 15 min later after dispersion. The superb dispersibility of the Q-MWNTs was beneficial to forming a uniform and stable film on GCE. Fig. 1B shows the SEM image of the Q-MWNTs film on the GCE. It can be seen that Q-MWNTs were efficiently entrapped onto the GCE surface mostly in the form of single tubes. It was believed that the single tubes would significantly activate the electrode surface and accelerate the electron transfer. In addition, electrostatic interactions occurred between the positively charged Q-MWNTs and the negatively charged anodized GCE surface as shown in Fig. 1C. Based on these, the Q-MWNTs/GCE can offer advantages such as high stability and homogeneousness for polymer immobilization.

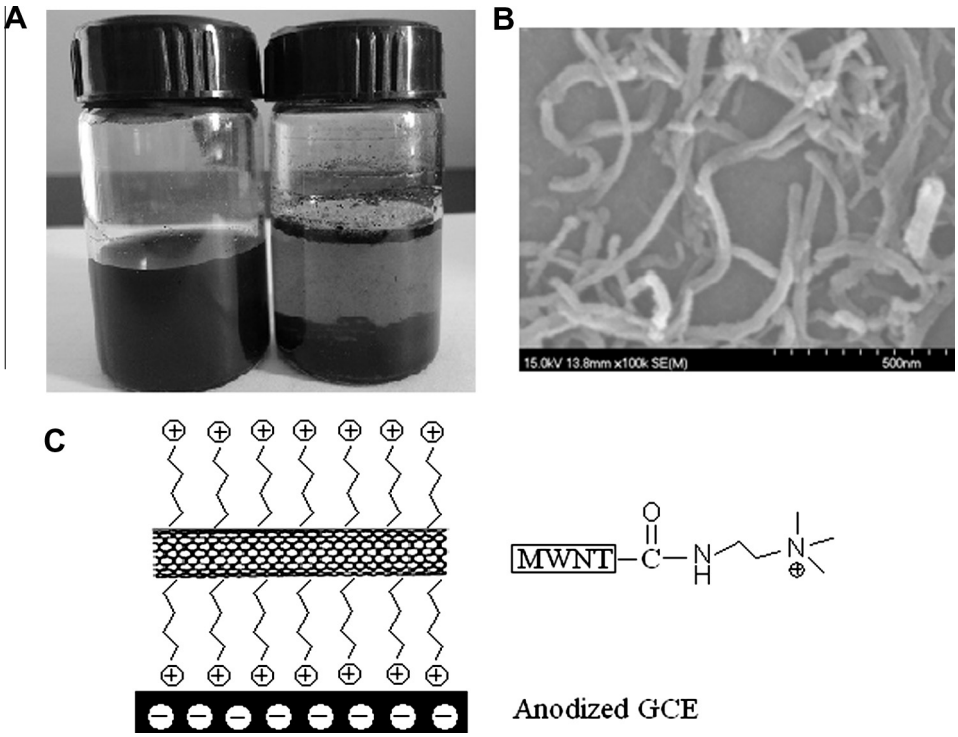

Fig. 1. (A) Digital images of Q-MWNTs (a) and MWNTs–COOH (b) in deionized water (1.0 mg mL^{-1}) 15 min later after dispersion. (B) SEM image of the Q-MWNTs. (C) Schematic representation of the procedure for fabricating Q-MWNTs/GCE.

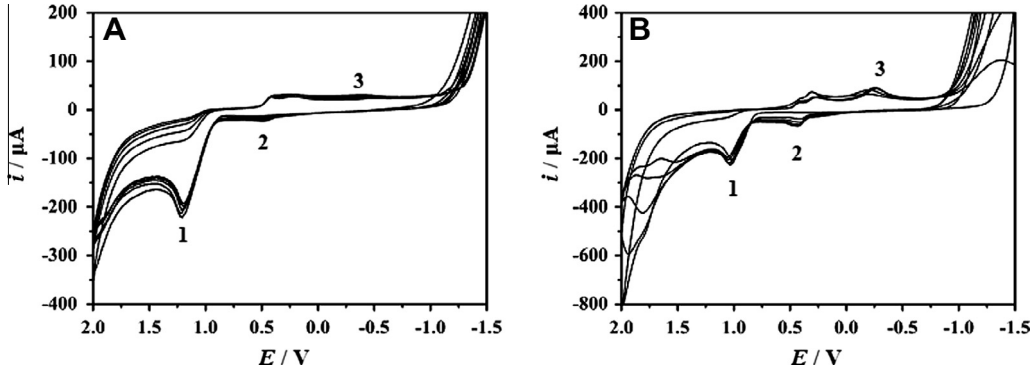

Fig. 2. Repetitive CVs of 0.01 M ABSA in 0.1 M H_2SO_4 at bare GCE (A) and Q-MWNTs/GCE (B). Scan rate: 0.05 V s^{-1}.

3.2. Electropolymerization of ABSA at the Q-MWNTs/GCE surface

Voltammograms of 0.01 M ABSA in 0.1 M H_2SO_4 at bare GCE and Q-MWNTs/GCE for 5 cycles are shown in Fig. 2. Anodic peak 1, 2 and cathodic peak 3 were observed at bare GCE (Fig. 2A) with peak potential value at +1.2, +0.5 and −0.4 V, respectively. Then, larger peaks were observed upon continuous scanning, reflecting the continuous growth of the film. Similar voltammograms with peak 1 (+1.0 V), peak 2 (+0.4 V) and peak 3 (−0.3 V) were obtained during the electropolymerization at Q-MWNTs/GCE (Fig. 2B). The electrochemical behavior of ABSA may be as follows [28,35]: ABSA was oxidized to free radical (peak 1) at first; the free radical combined rapidly to hydrazobenzene sulfonic acid; then hydrazobenzene sulfonic acid was oxidized to azobenzene sulfonic acid (peak 2), and azobenzene sulfonic acid reduced to hydrazobenzene sulfonic acid (peak 3). Compared with the voltammograms at bare GCE, lower oxidation potentials and larger peak currents were obtained at Q-MWNTs/GCE, indicating that PABSA film was more easily electrodeposited on the Q-MWNTs surface. This could be ascribed to the large surface area of CNTs and electrostatic adsorption of ABSA (negatively charged sulfonic group) to the surface of positively charged Q-MWNTs. Besides, anodic peak (from +1.8 to +2.0 V) and cathodic peak (+0.3 V) were also observed upon continuous scanning at Q-MWNTs/GCE. This was probably due to the oxidation and reduction of the residual amino-groups of Q-MWNTs.

3.3. Characterization of modified electrode

EIS was used to characterize the electron transfer property of the modified electrodes. Fig. 3 shows the Nyquist plot of bare GCE (curve a), Q-MWNTs/GCE (curve b), PABSA/GCE (curve c) and PABSA/Q-MWNTs/GCE (curve d) in a solution containing 0.1 M KCl and 5 mM $K_3[Fe(CN)_6]/K_4[Fe(CN)_6]$. As shown in Fig. 3, there was a small semicircle of the Nyquist plot at high frequencies for bare GCE, implying that there was low electron transfer resistance to the redox-probe. After Q-MWNTs were immobilized on

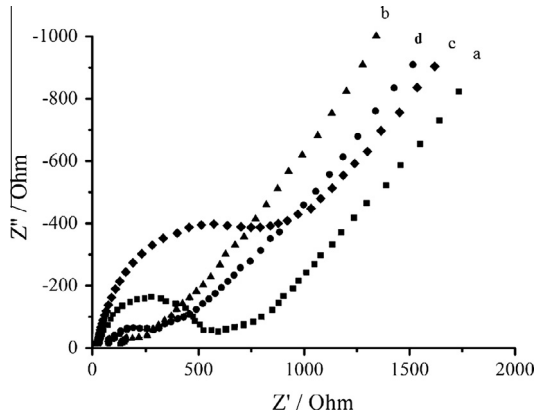

Fig. 3. EIS of bare GCE (curve a), Q-MWNTs/GCE (curve b), PABSA/GCE (curve c) and PABSA/Q-MWNTs/GCE (curve d) recorded in 0.1 M KCl solution containing 5 mM $[Fe(CN)6]^{3-/4-}$.

GCE, it was observed that the diameter of the semicircle plot decreased largely. This result demonstrated that Q-MWNTs present on GCE facilitated the electron-transfer process of redox-probe on the electrode surface. After modification with polymer, the resistance of PABSA/GCE became larger at higher frequencies compared with that of bare GCE. The reason should be the large repulsion effect between the negatively charged $[Fe(CN)_6]^{3-/4-}$ and the negatively charged polymer film. The semicircle part plot of the composite film modified electrode was observed between curve a and curve b. The much smaller electron transfer resistance could be due to the accelerated electron-transfer of CNTs and charge neutralization between PABSA and Q-MWNTs.

3.4. Electrochemical behaviors of MTX and CF at modified electrode

Representative CVs of pH 7.0 PBS at the bare GCE (Fig. 4A), Q-MWNTs/GCE (Fig. 4B), PABSA/GCE (Fig. 4C) and PABSA/Q-MWNTs/GCE (Fig. 4D) with the absence (curve a) and presence (curve b) of 20 μM MTX were shown. Broad peaks ranged from +0.7 to +1.0 V was observed for MTX oxidation at both bare GCE and PABSA/GCE. At the Q-MWNTs/GCE, a distinct anodic peak was observed for MTX at +0.80 V and the peak current increased. This indicated that the oxidation process of MTX was greatly improved by the Q-MWNTs. Fig. 4D strongly suggested that the composite film can combine the advantages of both. The enhancement of the peak current and the lowered oxidation overpotential (+0.72 V) in contrast to PABSA and Q-MWNTs are clear evidences of the synergistic effect of both. CF also had a distinct oxidation peak (+0.46 V) at the PABSA/Q-MWNTs/GCE (Fig. 4H). The oxidation current was higher and the oxidation overpotential was lower than that at the bare GCE (Fig. 4E), Q-MWNTs/GCE (Fig. 4F) and PABSA/GCE (Fig. 4G). PABSA film is consisted of many high conjugated dimer molecules and has the ability to interact with many components through hydrogen bonding and π–π stacking. Both MTX and CF have three aromatic rings. They can be adsorbed to the polymer surface through π–π stacking between the aromatic rings and the dimers. On the other hand, the stacking of conjugated aromatic rings might provide a perfect pathway for charge transport from the MTX and CF molecules to the electrode and facilitate the electron transfer processes. Therefore, enhanced peak current responses and lower oxidation peak potentials of MTX and CF were obtained after PABSA film was immobilized on the Q-MWNTs/GCE surface, which indicated that the composite film can significantly accelerate the electron-transfer process and catalyze the electrochemical oxidation of MTX and CF. The peak-to-peak separation for MTX and CF is 0.26 V at the PABSA/Q-MWNTs/GCE in CVs. Clearly MTX and CF can be distinguished effectively at the PABSA/Q-MWNTs/GCE.

3.5. Selection of the experimental conditions

3.5.1. Effect of pH

The pH of the supporting electrolyte had a substantial effect on the oxidation potentials and currents of MTX and CF. The CVs of MTX and CF at the PABSA/Q-MWNTs/GCE in PBS with pH varying from 3.0 to 8.0 were shown in Supplementary data of Fig. 1S. Both the anodic peak potentials (E_{pa}) of MTX and CF shifted negatively with increasing solution pH value, suggesting that protons participated in the electrode reaction. The relationships between the anodic peak potentials and pH for MTX and CF followed the equations E_{pa} (V) = 1.1375–0.0519 pH (r = 0.9989) and E_{pa} (V) = 0.8019–0.046 pH (r = 0.9987), respectively. The slopes of the regression equations are close to the theoretical value of 59 mV/pH. Such behavior suggests that it obeys the Nernst equation for an equal electron and proton exchange process in the oxidation reaction of MTX and CF [36]. With the increase of pH value, the anodic peak currents of MTX increased until the pH value reached 5.0 and then decreased. The anodic peak currents of CF also increased with the increase of pH value from 3.0 to 7.0. The anodic peak currents decreased rapidly when the pH value is higher than 7.0. In the following experiments, pH 7.0 PBS was chosen for the electrochemical determination of MTX and CF since it is close to the pH of physiological condition.

3.5.2. Effect of scan rate

To elucidate the electrode reaction at the modified electrode, the influence of scan rate (v) on the elecrocatalytic properties of the PABSA/Q-MWNTs/GCE was studied by cyclic scanning MTX and CF in pH 7.0 PBS with different scan rates ranging from 0.005 to 0.45 V s^{-1}. The anodic peak currents (i_{pa}) of MTX and CF grew with increasing v, and there were good linear relationships between i_{pa} and square roots of scan rate ($v^{1/2}$) (shown in Supplementary data of Figs. 2S and 3S), indicating that the oxidation of MTX and CF at the PABSA/Q-MWNTs/GCE followed a diffusion-controlled mechanism. Furthermore, the oxidation peak potentials (E_{pa}) of MTX and CF shifted positively with the increasing v, which means that the electrochemical reaction is irreversible. Good linear relationships were observed between E_{pa} (V) and logarithm of the scan rate ($\log v$) for both MTX and CF (shown in Supplementary data of Figs. 2S and 3S). For an irreversible electrode reaction, the relationship between E_{pa} and $\log v$ follows the equation [37]: $E_p = -K + (2.303RT/2(1-\alpha)nF)\ \log v$. Thus, the obtained transfer coefficients (α) for MTX and CF oxidation are equal to 0.64 and 0.63, respectively.

3.6. Simultaneous determination of MTX and CF

Differential pulse voltammetry (DPV) was performed to investigate the relationship between the peak current and concentration of MTX and CF due to its higher sensitivity. The individual determination of MTX or CF in their mixtures was performed by changing the concentration of one species while keeping the other constant. Fig. 5A shows the differential pulse voltammograms (DPVs) of different concentrations of MTX in pH 7.0 PBS with a constant CF concentration of 8.0 μM. The results showed that the anodic peak current was proportional to the concentration of MTX from 0.1 to 8.0 μM. The regression equation was i_{pa} (μA) = 0.5111C (μM) + 0.119 with a correlation coefficient of 0.9990, and the detection limit (LOD) was 0.015 μM with a signal-to-noise ratio (S/N) of 3. Similarly, as shown in Fig. 6A, when keeping the concentration of MTX constant at 8.0 μM, the anodic peak current of CF increased linearly with its concentration from 0.1 to 6.5 μM. A lin-

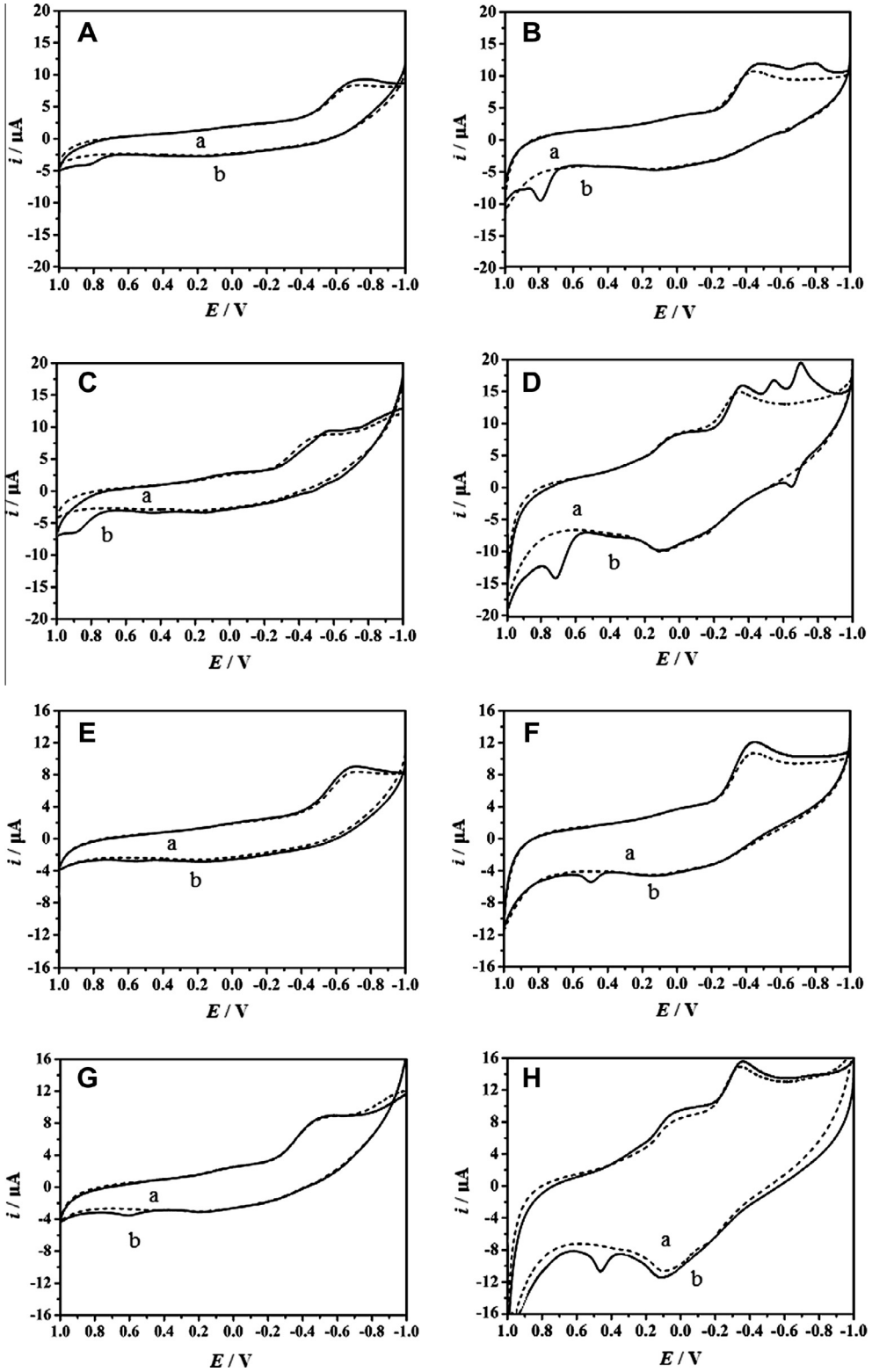

Fig. 4. CVs of the bare GCE (A, E), Q-MWNTs/GCE (B, F), PABSA/GCE (C, G) and PABSA/Q-MWNTs/GCE (D, H) in pH 7.0 PBS with the absence (a) and presence (b) of 20 μM MTX (A, B, C, D) and CF (E, F, G, H). Scan rate: 0.05 V s^{-1}.

ear equation i_{pa} (μA) = 0.5483C (μM) + 0.0034 with a correlation coefficient of 0.9981 was obtained and the LOD was 0.020 μM. All these experimental results showed that our proposed method allowed sensitive and simultaneous determination of MTX and CF without interference of each other. The presented method with a simple electrode preparation can provide comparable detection limits with other previous methods (shown in Table 1). In addition, compared with other methods, our proposed electrochemical method offered several advantages, such as its simplicity, high sensitivity, good stability and low-cost instrumentation.

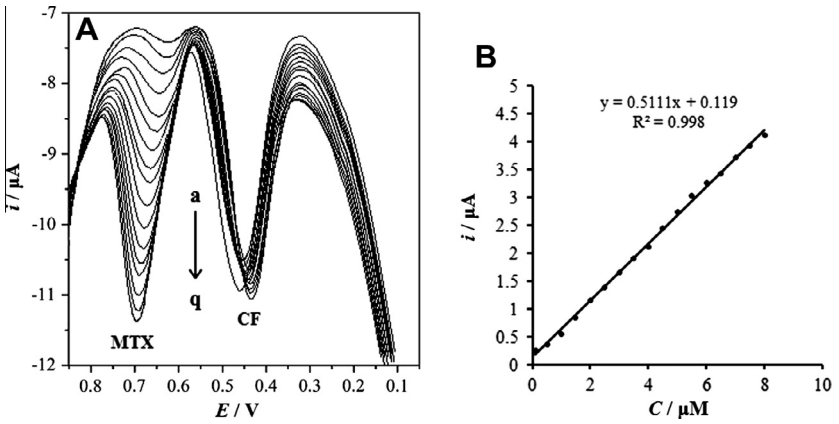

Fig. 5. (A) DPVs of the PABSA/Q-MWNTs/GCE in the presence of 8.0 μM CF containing different concentrations of MTX (a-q: 0.1, 0.5, 1.0, 1.5, 2.0, 2.5, 3.0, 3.5, 4.0, 4.5, 5.0, 5.5, 6.0, 6.5, 7.0, 7.5 and 8.0 μM) in pH 7.0 PBS. (B) The relationship of current responses with the concentrations of MTX.

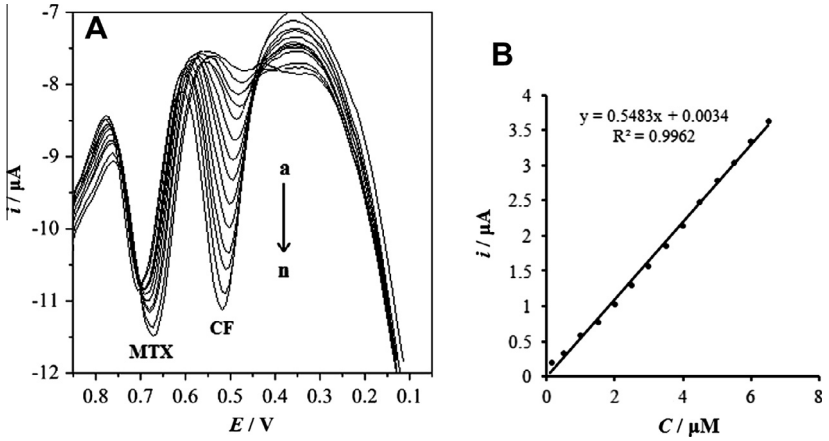

Fig. 6. (A) DPVs of the PABSA/Q-MWNTs/GCE in the presence of 8.0 μM MTX containing different concentrations of CF (a-n: 0.1, 0.5, 1.0, 1.5, 2.0, 2.5, 3.0, 3.5, 4.0, 4.5, 5.0, 5.5, 6.0 and 6.5 μM) in pH 7.0 PBS. (B) The relationship of current responses with the concentrations of CF.

Table 1
Comparison of some methods for the determination of MTX and CF.

Separation	Detection	LOD (μM)		Ref.
		MTX	CF	
CE	UV	1.0	—	[12]
HPLC	fluorescence	6.1	—	[13]
HPLC	UV	6.6	—	[14]
HPLC	fluorescence	16.5	—	[15]
HPLC	fluorescence	—	9.8	[16]
HPLC	UV	—	19.6	[17]
CE	UV	0.86	0.76	[18]
LC	ESI-MS	0.007	0.006	[19]
Voltammetry	0.015	0.02	This work	

3.7. Reproducibility and stability of the PABSA/Q-MWNTs/GCE

The reproducibility of the PABSA/Q-MWNTs/GCE was examined by the detection of 5.0 μM MTX in pH 7.0 PBS for six successive determinations by DPV. The relative standard deviation (RSD) of the oxidation peak currents was 2.4%, showing that the PABSA/Q-MWNTs/GCE had good reproducibility. The stability of the PABSA/Q-MWNTs/GCE was also investigated. The peak currents decreased by 4.4% after 1 week storage at 4 °C. After 3 weeks, the current response was approximately 90% of the originally measured value. The excellent reproducibility and long-term stability of the PABSA/Q-MWNTs/GCE make them attractive in the fabrication of electrochemical sensors.

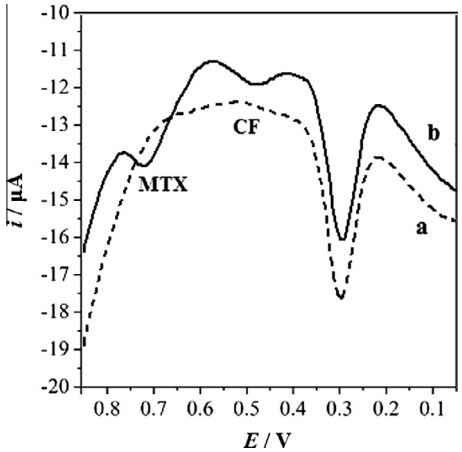

Fig. 7. DPVs obtained for blank urine (a) and spiked urine with the addition of 1.5 μM MTX and 0.5 μM CF (b) at the PABSA/Q-MWNTs/GCE in pH 7.0 PBS.

3.8. Interference of coexisting substances

The influence of various substances on the determination of 5.0 μM MTX and CF was studied by DPV. It is found that 1000-fold Na^+, K^+, NH_4^+, Ca^{2+}, Mg^{2+}, Cl^-, $NO3^-$, SO_4^{2-} and 100-fold ascorbic acid, uric acid, glucose, tartaric acid and citric acid do not interfere

Table 2
Recovery results for MTX and CF in urine samples.

Sample no.	Added (μM)		Found[a] (μM)		Recovery (%)		RSD (%)	
	MTX	CF	MTX	CF	MTX	CF	MTX	CF
1	1.5	0.5	1.61	0.53	107.3	106.0	2.6	1.8
2	0.5	1.5	0.47	1.43	94.0	95.3	1.9	2.7
3	1	1	0.95	1.08	95.0	108.0	1.4	1.1
4	5.0	5.0	4.92	5.11	98.4	102.2	1.6	1.2

[a] Average of three determinations.

with the determination and the tolerance limit was estimated to be less than 5% of the relative error, indicating an excellent anti-interference ability of our proposed method.

3.9. Analytical applications

To investigate the applicability of the proposed method for simultaneous determinations of MTX and CF, urine samples without any pretreatment were used for quantitative analysis. Since MTX and CF were not contained in healthy human urine samples, the spike and recovery experiments were performed by measuring the DPV responses to urine samples in which known concentrations of MTX and CF were added. Fig. 7 shows representative DPVs of blank (curve a) and spiked (curve b) urine samples with the addition of 1.5 μM MTX and 0.5 μM CF. The amounts of MTX and CF in the urine samples were then determined by calibration method and were summarized in Table 2. The recoveries were 94.0–107.3% and 95.3–106.0% for MTX and CF, respectively, which clearly indicated the applicability and reliability of our proposed method.

4. Conclusion

In this work, we have successfully developed an electrochemical method for direct simultaneous determination of MTX and CF by using DPV at the PABSA/Q-MWNTs/GCE. Well-defined peaks and significant increase of peak currents were observed for MTX and CF at the PABSA/Q-MWNTs/GCE, which clearly demonstrated that the composite film could be used as an efficient promoter to enhance the kinetics of the electrochemical process of MTX and CF. The well-distinguished two anodic peaks of MTX and CF at the PABSA/Q-MWNTs/GCE showed that simultaneous determination of them was possible. So, it was used for quantitative determination of MTX and CF in urine samples with high sensitivity and selectivity.

Acknowledgements

This is a project supported by Major National Scientific Instrument and Equipment Development Special of China (Nos. 2012YQ090229, 2012YQ09022903), National Natural Science Foundation of China (No. 20775070) and Zhejiang Provincial Natural Science Foundation of China (Nos. Y407153, Y4100190), and also sponsored by Zhejiang Provincial Assay Foundation of China (Nos. 2012C37003, 2012C37007).

Appendix A. Supplementary material

Supplementary data associated with this article can be found, in the online version, at http://dx.doi.org/10.1016/j.jelechem.2013.09.004.

References

[1] J.C. Panetta, A. Wall, C.H. Pui, M.V. Relling, W.E. Evans, Clin. Cancer Res. 8 (2002) 2423–2429.
[2] J.M. Kremer, Ann. Intern. Med. 134 (2001) 695–706.
[3] E. Tanaka, A. Taniguchi, W. Urano, H. Yamanaka, N. Kamatani, Best Pract. Res. Cl. Rh. 18 (2004) 233–247.
[4] A.V. Ramanan, P. Whitworth, E.M. Baildam, Arch. Dis. Child. 88 (2003) 197–200.
[5] R.L. Blakley, S.J. Benkovic (Eds.), Folates and Pteridines, vol. 1, Wiley-Interscience, New York, 1984.
[6] M.G. Nair, in: D.E.V. Wilman (Ed.), Chemistry of Antitumor Agents, Blackie, New York, 1990, pp. 202–233.
[7] E. Mini, J.R. Bertino, in: T.C. Chou, D.C. Rideout (Eds.), Synergism and Antagonism in Chemotherapy, Academic Press Inc., SanDiego, 1991, pp. 449–506.
[8] T. CercosFortea, V.G. Casabo, A. Nacher, E. CejudoFerragud, A. Polache, M. Merino, Int. J. Pharm. 155 (1997) 109–119.
[9] Y. Finkelstein, S. Zevin, J. Heyd, Y. Bentur, Y. Zigelman, M. Hersch, Neurotoxicology 25 (2004) 407–410.
[10] M.A. Pesce, S.H. Bodourian, Ther. Drug Monit. 8 (1986) 115–121.
[11] V. Raso, R. Schreiber, Cancer Res. 35 (1975) 1407–1410.
[12] C.Y. Kuo, H.L. Wu, H.S. Kou, S.S. Chiou, D.C. Wu, S.M. Wu, J. Chromatogr. A 1014 (2003) 93–101.
[13] S. Emara, S. Razee, A. Khedr, T. Masujima, Biomed. Chromatogr. 11 (1997) 42–46.
[14] A. Sparreboom, W.J. Loos, K. Nooter, G. Stoter, J. Verweij, J. Chromatogr. B 735 (1999) 111–119.
[15] E.D. Lobo, J.P. Balthasar, J. Chromatogr. B 736 (1999) 191–199.
[16] E. Schleyer, J. Reinhardt, M. Unterhalt, W. Hiddemann, J. Chromatogr. B 669 (1995) 319–330.
[17] G.L. Duan, L.X. Zheng, J. Chen, W.B. Cheng, D. Li, Biomed. Chromatogr. 16 (2002) 282–286.
[18] J.R. Flores, G.C. Penalvo, A.E. Mansilla, M.J.R. Gomez, J. Chromatogr. B 819 (2005) 141–147.
[19] P. Koufopantelis, S. Georgakakou, M. Kazanis, C. Giaginis, A. Margeli, S. Papargiri, I. Panderi, J. Chromatogr. B 877 (2009) 3850–3856.
[20] S. Iijima, Nature 354 (1991) 56–58.
[21] H.X. Luo, Z.J. Shi, N.Q. Li, Z.N. Gu, Q.K. Zhuang, Anal. Chem. 73 (2001) 915–920.
[22] J.X. Wang, M.X. Li, Z.J. Shi, N.Q. Li, Z.N. Gu, Electrochim Acta 47 (2001) 651–657.
[23] J. Wang, M. Musameh, Y.H. Lin, J. Am. Chem. Soc. 125 (2003) 2408–2409.
[24] K.P. Gong, Y. Dong, S.X. Xiong, Y. Chen, L.Q. Mao, Biosens. Bioelectron. 20 (2004) 253–259.
[25] Y.Z. Wang, Q. Li, S.S. Hu, Bioelectrochemistry 65 (2005) 135–142.
[26] R.S. Chen, W.H. Huang, H. Tong, Z.L. Wang, J.K. Cheng, Anal. Chem. 75 (2003) 6341–6345.
[27] S. Wang, Z.Q. Qi, H.K. Huang, H. Ding, Anal. Lett. 45 (2012) 1658–1669.
[28] F. Xu, M.N. Gao, L. Wang, G.Y. Shi, W. Zhang, L.T. Jin, J.Y. Jin, Talanta 55 (2001) 329–336.
[29] H. Tang, G.Z. Hu, S.X. Jiang, X. Liu, J. Appl. Electrochem. 39 (2009) 2323–2328.
[30] S.A. Kumar, S.M. Chen, J. Mol. Catal. A, Chem., A, Chem. 278 (2007) 244–250.
[31] K.J. Huang, D.F. Luo, W.Z. Xie, Y.S. Yu, Colloid Surf. B 61 (2008) 176–181.
[32] G.Y. Jin, F. Huang, W. Li, S.N. Yu, S. Zhang, J.L. Kong, Talanta 74 (2008) 815–820.
[33] F. Huang, G.Y. Jin, Y. Liu, J.L. Kong, Talanta 74 (2008) 1435–1441.
[34] M. Ghosh, S. Maiti, S. Dutta, D. Das, P.K. Das, Langmuir 28 (2012) 1715–1724.
[35] G.Y. Jin, Y.Z. Zhang, W.X. Cheng, Sens. Actuator B: Chem. 107 (2005) 528–534.
[36] A.J. Bard, L.R. Faulkner, Electrochemical Methods: Fundamentals and Applications, 2nd ed., Wiley, New York, 2001.
[37] G. Erdogdu, A.E. Karagozler, Talanta 44 (1997) 2011–2018.